Synthesis and Characterization of Polypyrrole Rod Doped with *p*-Toluenesulfonic Acid via Micelle Formation

Duk Ki Kim,[1] Kyung Wha Oh,[2] Hee Jun Ahn,[1] Seong Hun Kim[1]

[1]*Department of Fiber and Polymer Engineering, Hanyang University, Sungdong-gu, Seoul 133-791, Korea*
[2]*Department of Home Economics Education, Chungang University, Dongjak-gu, Seoul 156-756, Korea*

Received 5 January 2007; accepted 30 September 2007
DOI 10.1002/app.27509
Published online 10 December 2007 in Wiley InterScience (www.interscience.wiley.com).

ABSTRACT: Rod-type polypyrrole (PPY) doped with *p*-toluenesulfonic acid (TSA) was synthesized by chemical oxidative polymerization via a self-assembly process. The shape of the PPY particles is mainly determined by the ratio of TSA/pyrrole (PY) and feed rate of the oxidant. Particle of different shapes (rod, grain, and partially rod) exhibit differences in morphology, electrical properties, dispersity, and thermal properties. Wide-angle X-ray diffraction patterning analysis was used to investigate the mechanism of rod formation. The effect of the TSA concentration on the PPY structure was investigated using Fourier transform infrared spectroscopy. The PPY rods doped with TSA exhibited better electrical conductivity than granular PPY doped with TSA, and their dispersity and thermal stability were also higher. Self-orientation of PPY in the micelles of TSA and high crystallinity of the rod particles led to improved thermal stability. Hence, the decomposition temperature of the polymer chain was considerably increased. © 2007 Wiley Periodicals, Inc. J Appl Polym Sci 107: 3925–3932, 2008

Key words: polypyrroles; surfactants; conducting polymers; *in situ* doping polymerization

INTRODUCTION

Since polyacetylene was reported by Shirakawa et al. in 1977,[1] conducting polymers containing conjugated structures have been studied because of their intrinsic electrical conductivity at room temperature and potential use for electronic devices. Polypyrrole (PPY) is a particularly promising material; it has relatively high conductivity, good environmental stability, and it is easy to polymerize.[2] Recently, conducting nano/micro materials based on PPY or polyaniline have attracted interests of many researchers.[3–5] Such nanomaterials are applicable in various electronic devices, such as conducting films, obtained by solvent casting; polymer electrodes, obtained by blending; and conducting fillers of electromagnetic shielding materials.[6–11] In these applications, conducting particles must exhibit dispersion stability over long periods, and maintain their electrical conductivity. The patterning of conducting polymer circuits by lithography or mold compressing methods has been studied.[12,13] For processes using heat, such as mold compression patterning, thermal stability at the processing temperature is required.

Two kinds of polymerization methods, electrochemical polymerization and chemical oxidative polymerization, are generally used to synthesize conducting polymers. The electrochemical method generally synthesizes conducting polymers in the form of films. Sometimes template methods have been used to prepare the conducting nanotubes or nanowires.[11,14] However, these types of particles are not suitable for conducting filler in polymer substrate. Therefore, the preparation of self-assembled particles of nano- or microsized conducting polymers by emulsion polymerization using organic surfactants has been investigated.[15,16] Previously, various organic surfactants such as naphthalenesulfonic acid (NSA), dodecylbenzenesulfonic acid (DBSA), and camphorsulfonic acid (CSA) have been used.[17–20] It was found that the morphology and size of the conducting particles were affected by the types and concentrations of the surfactants used.[21,22] In the self-assembly system described in this article, the acid dopant acts also as the template, by micelle formation. Of the various available surfactants, *p*-toluenesulfonic acid (TSA) was selected because of its efficiency. TSA is a highly water-soluble, commercial surfactant, with a small hydrophobic group. These properties are advantageous for micelle formation. The solubility of other surfactants in water, such as DBSA, NSA, is very low, requiring long periods of magnetic stirring, or ultra-sonification. TSA dissolves readily, requiring only magnetic stirring. Emulsions formed from TSA exhibit highly dense structures

Correspondence to: S. H. Kim (kimsh@hanyang.ac.kr).
Contract grant sponsor: Hanyang University; contract grant number: HY-2006-I.

Journal of Applied Polymer Science, Vol. 107, 3925–3932 (2008)

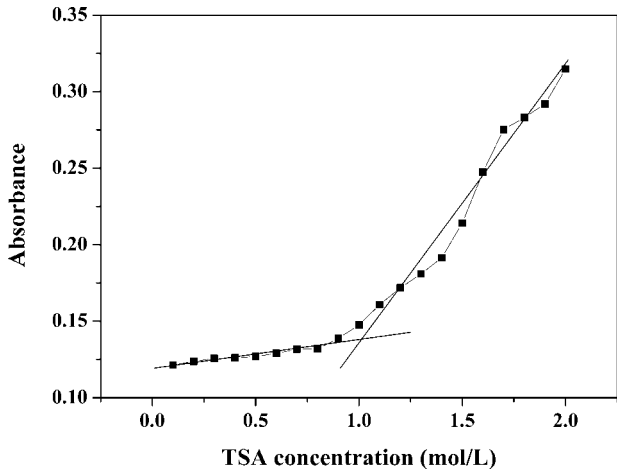

Figure 1 The UV–vis absorbance (wavelength: 380 nm) of aqueous TSA solutions of various concentrations at 0°C.

because the TSA occupies a relatively small space on a micelle compared with other ionic surfactants. Under high-voltage conditions, the decomposition of conducting fillers by heat generation is a serious problem. The property of high density, induced by TSA should improve the thermal stability of PPY.

The purpose of this study is to synthesize conducting particles that have excellent dispersity, derived from the essential hydrophilic property of $-SO_3$ in TSA, and thermal stability and chemical stability, emanating from the dense structure of TSA.[23,24] The synthesized rod-shaped PPY (PPY rod) satisfied these requirements. In this article, the relationship between polymerization conditions and other properties such as electrical conductivity, morphology, dispersity, and thermal stability will be discussed and the optimum conditions for the formation of PPY rods will be proposed.

EXPERIMENTAL

Materials

Pyrrole monomer (PY), TSA as a surfactant, and ammoniumpersulfate (APS) as an oxidant were purchased from Aldrich, St. Louis, MO. PY monomer, with a high degree of purity, was used as received. The critical micelle concentration (cmc) of TSA was measured by a light scattering method.[24] Absorption intensity of each sample at wavelength 380 nm of visible light region was measured using SCINCO *S*-4100 UV–vis spectrometer. Figure 1 shows that the curve of turbidity against TSA concentration exhibits discontinuity near the cmc. A sudden increase in turbidity means that the TSA molecules set, to form micelles. The cmc of TSA was $\sim 1.0M$.

Synthesis

The conducting PPY doped with TSA was synthesized by chemical oxidative polymerization, via a self-assembly process. TSA was added to 100 mL deionized water, with magnetic stirring. After stirring for 1 h, PY monomer was slowly added to the TSA solution through a syringe. To determine the effect of the TSA/PY monomer ratio, the concentration of added PY monomer was fixed at $0.7M$, and the ratios of TSA/PY monomer were varied as follows: 0.5, 1.0, 1.5, 2.0, and 2.5. After stirring for 3 h, separate aqueous solution of APS (100 mL), with the same as the monomer ($0.7M$), were added to each of the surfactant/monomer solutions. To investigate the effect of the feed rate of the oxidant on the morphology, and the doping effect of the synthesized particles, the feed rate and time of the oxidant were varied. The reaction temperature was fixed at 0°C. Oxidant was fed at a rate of either 16.6 mL/h for 6 h or at 6.25 mL/h for 16 h. After polymerization, excess methanol was added to the PPY dispersion to precipitate PPY powder by disrupting the hydrophile–lypophile balance of the system and terminating the reaction. After filteration under reduced pressure, the precipitated PPY particles were collected on a glass filter. They were then washed with methanol and deionized water three times to remove any unreacted PY monomer and oxidant. The resultant particles were dried *in vacuo* at 40°C for 48 h.

Characterization

Field-emission scanning electron microscopy (FE-SEM; JEOL JSM-6330F, Tokyo, Japan) was used to determine the morphology of the prepared PPY. To confirm an increase in crystallinity and self-orientation of the PPY chains, wide-angle X-ray diffraction (WAXD) data were collected with a Rigaku Denki D-Max2000 instrument. The electrical conductivity of PPY doped with TSA was measured by means of a four-probe method, using a Keithly 238 high-current-source measuring unit at room temperature.[25] The electrical conductivity was calculated using eq. (1)

$$\sigma(\mathrm{S/cm}) = \frac{\ln 2}{\pi t} \times \frac{I}{E} \approx 0.22/t \times \frac{I}{E} \qquad (1)$$

where, σ is electrical conductivity; t is the thickness of sample; E is the voltage drop across the inner probes; and I is the current passing through the outer probes. The Fourier transform infrared (FTIR) spectra of PPY doped with TSA were recorded with a Nicolet 760 Magna IR spectrometer, using KBr discs. Existence of TSA as dopant and the influence of dedoping and redoping treatment were observed

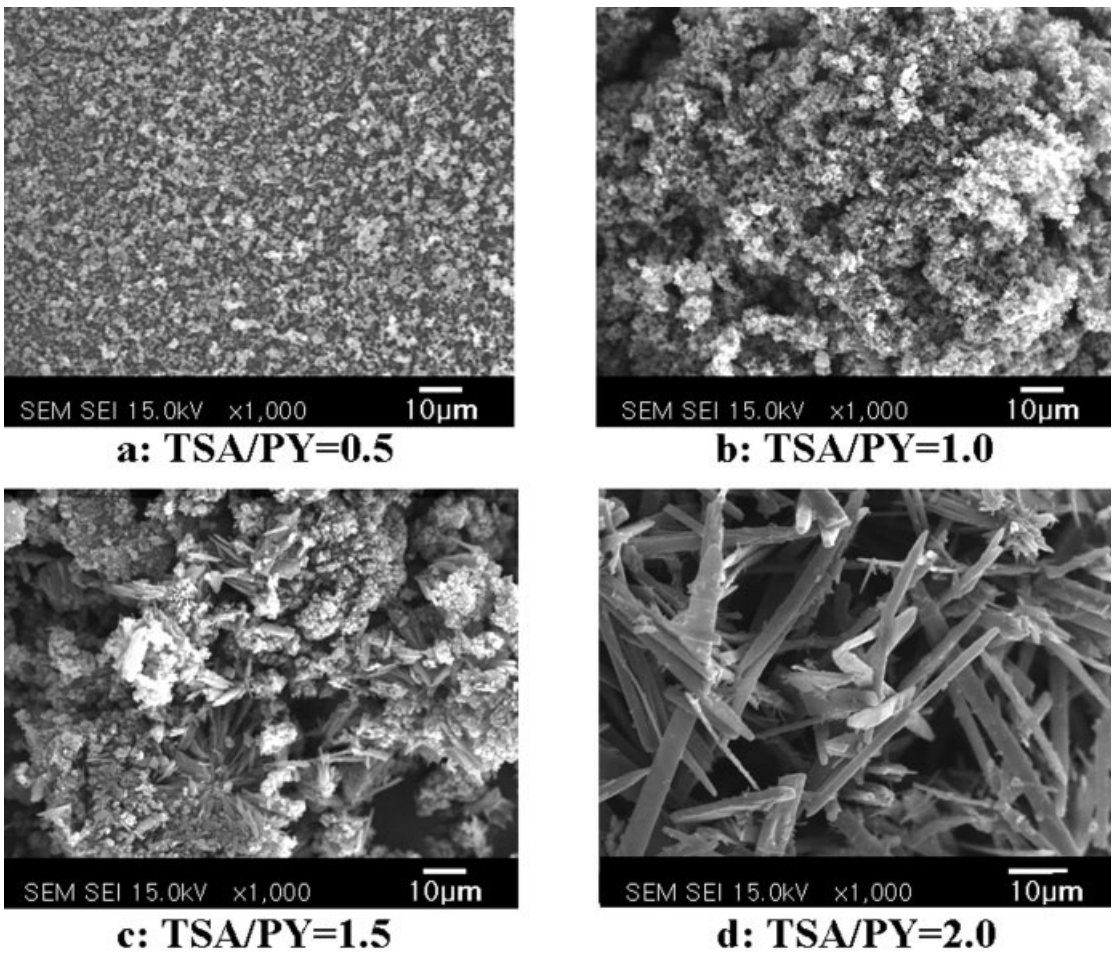

Figure 2 Changes in morphology of PPY doped with TSA, according to the ratio of TSA/pyrrole at an oxidant feed rate of 6.25 mL/h.

through UV–vis spectra using SCINCO *S*-4100 UV–vis spectrometer.[26] To investigate the dispersity of the particles, they were applied to *m*-cresol and the dispersive stability was observed after 48 h. The compatibility of particles with Nafion® was determined by a solvent casting method. TGA/mass spectroscopy (TG209 F1-FTIR-MS) was used to determine the thermal stability of the PPY particles and ele-

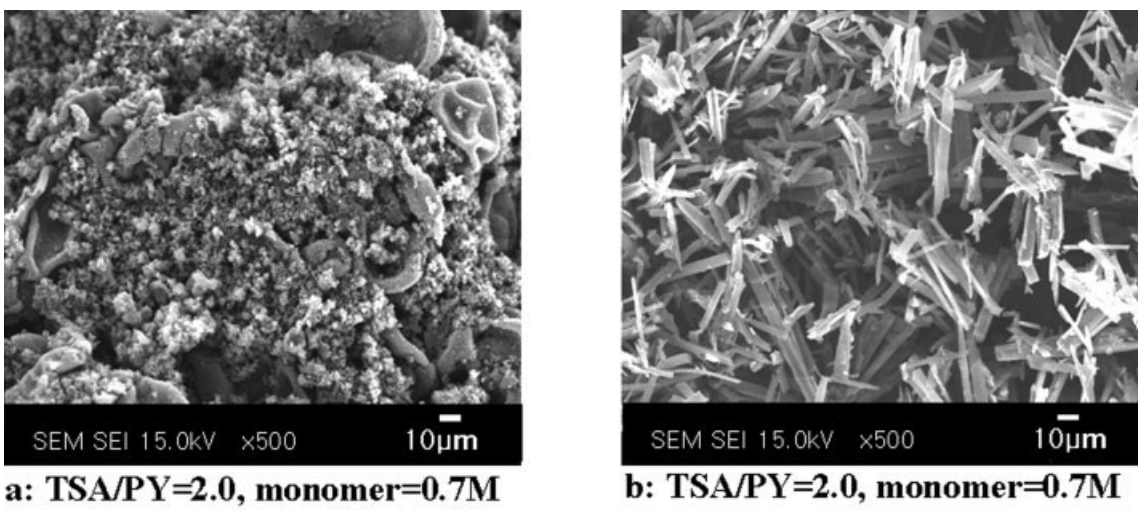

Figure 3 Changes in morphology of PPY doped with TSA, according to oxidant feeding time: (a) 6 h (feed rate, 16.6 mL/h) and (b) 16 h (feed rate, 6.25 mL/h).

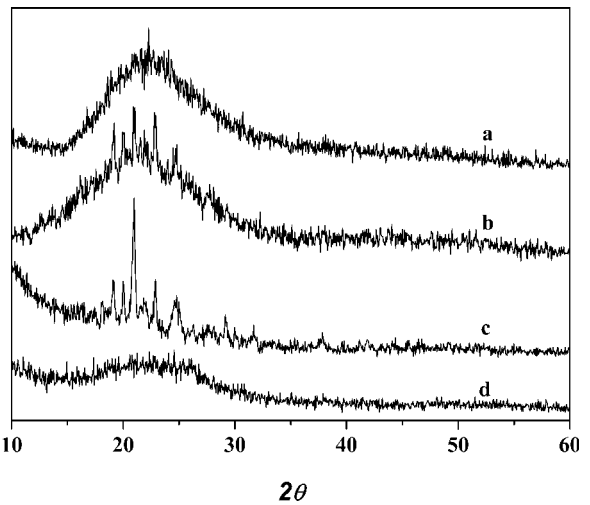

Figure 4 X-ray scattering patterns of PPY doped with TSA synthesized under the following conditions: (a) TSA/PPY = 0.5, (b) TSA/PPY = 1.5, (c) TSA/PPY = 2.0, and (d) dedoping rod-type with $NH_3 \cdot H_2O$ (3 mol/L).

ments of the gas phase upon thermal decomposition. For the thermal analysis, the temperature was increased from room temperature to 1000°C at the rate of 10°C/min.

RESULTS AND DISCUSSION

Morphology

Various morphologies of PPY doped with TSA were observed, depending on the molar ratio of TSA/PY and the oxidant feed rate. First, the effect of the TSA/PY ratio on the morphological changes of PPY doped with TSA was investigated. This was done using an oxidant feed rate of 6.25 mL/h and an initial PY monomer concentration of 0.7*M*. Figure 2 shows that a granular morphology appeared when a TSA/PY molar ratio of less than 1.0 was used. The average diameter of granular PPY was estimated to be ~700 nm. A partially rod-shaped PPY appeared as the TSA/PY molar ratio was increased to 1.5*M*. When the TSA/PY ratio was 2.0, the shape of the particles of PPY doped with TSA was rod-like. The width and length of PPY rods were estimated to be 0.5–2 μm and 10–80 μm.

The oxidant feed rate also has an effect on the morphology of PPY. Figure 3(b) shows that PPY rods were formed at a slow feed rate. However, phase separation between TSA crystals and PPY occurred when the oxidant feed rate was high, as shown in Figure 3(a). It is assumed that the rate of initiation was increased at the faster feeding rate of APS. A large number of radicals penetrated into micelles for a short period of time, and hence particle growth in the longitudinal direction becomes difficult. It is expected that this fast feed of oxidant has

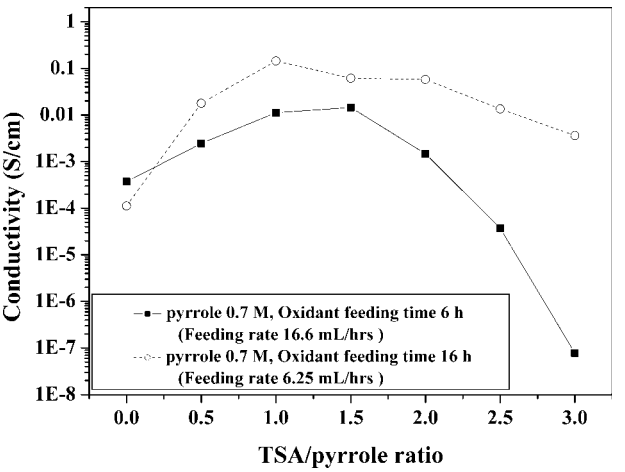

Figure 5 Electrical conductivity at room temperature of PPY doped with TSA, synthesized using various oxidant feed rates and times.

a considerable influence on the large decrease in electrical conductivity because of a low doping level of TSA due to coagulation of the PPY chain. Consequently, it is discussed as follows; longitudinal micelles formed by TSA molecules at concentrations over the cmc are maintained over all reaction times at slow oxidant feeds (6.25 mL/h), whereas with a fast oxidant feed (16.6 mL/h), the micelles of TSA could not form rod structures of PPY. Hence, the key factors that lead to the formation of rod-type PPY doped with TSA are the oxidant feed rate and the ratio of TSA/PY. However, the PPY rod particle sizes exhibited some degree of variation. Further research into control of the size of the rods is required to increase the electrical conductivity.

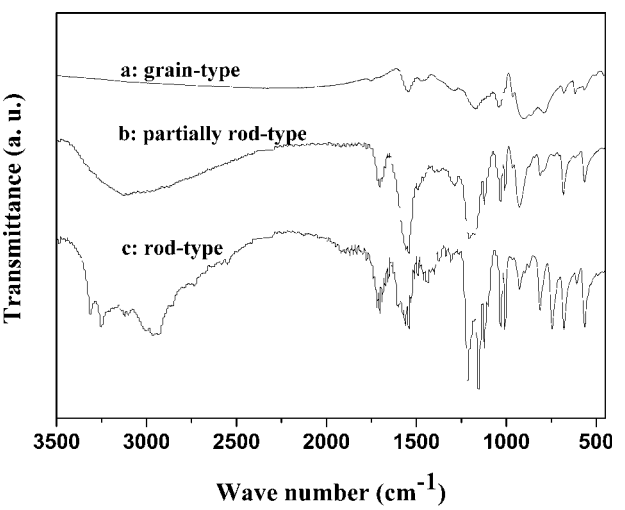

Figure 6 FTIR spectra of PPY doped with TSA synthesized at conditions of (a) TSA/PPY = 0.5, (b) TSA/PPY = 1.5, and (c) TSA/PPY = 2.0.

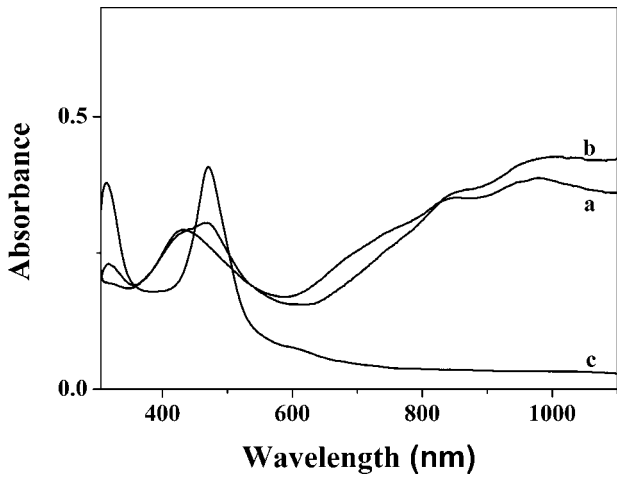

Figure 7 UV–vis spectra of (a) PPY doped with TSA synthesized at conditions of TSA/PPY = 2.0. (PPY rod), (b) PPY dedoped with $NH_3 \cdot H_2O$ (3 mol/L), and (c) PPY redoped with HCL (3 mol/L).

The XRD patterns shown in Figure 4 were identified using SEM images. In Figure 4(a), when the molar ratio of TSA/PY was 0.5, there was only one broad peak, centered at 22.5°, which means that most regions of synthesized PPY doped with TSA were amorphous. As the TSA/PY molar ratio increased, broad peaks representing amorphous regions disappeared. Further sharp peaks appeared at 19.2, 20.1, 21.9, 22.9 and 24.8°, in patterns. Consequently, this shows that an increase in the crystallinity of rod-type PPY arises by self-orientation, through TSA micelle formation.

Conductivity

Figure 5 shows that there is a significant relationship between the electrical conductivity and the TSA/PY molar ratio used in polymerization. The oxidant feed rate also affected the electrical conductivity of the product. The PPY synthesized via polymerization without using a surfactant exhibited a very low electrical conductivity of $\sim 10^{-4}$ S/cm. As the TSA/PY molar ratio increased up to 1.0, the electrical conductivity increased continuously, implying that TSA acts as a dopant, delocalizing the charge density of the PPY main chain. However, when the TSA/PY molar ratio exceeded 1.5, the electrical conductivity tended to gradually decrease under all polymerization conditions used. When different oxidant feed rates were used, vastly different electrical conductivities were recorded. Fast feed of oxidant disturbed the stable micelle formation causing the formation of PPY particles outside of the micelles. For slow feed rates of oxidant, it is proposed that TSA forms stable micelles containing PY monomers, and encloses the PPY polymer matrix after polymerization. This micelle formation mechanism was introduced by Wan and coworkers.[16] The FTIR spectra of PPY doped with TSA, as illustrated in Figure 6, show no significant differences from the spectra of PPY doped with other ionic surfactants.[26] Grain-type, rod-type, and partially rod-type samples were selected to compare the structures of the different products exhibiting different morphologies. The peaks related to the aromatic structure appeared in the region 1850–1650 cm^{-1}. The C=C stretching vibrations at both 1540 and 1440 cm^{-1} confirmed the existence of compounds containing aromatic rings. However, there are considerable differences in the absorption peaks in the region 3100–2850 cm^{-1}. In Figure 6(c), peaks for the aromatic rings and the C—H stretching vibrations band appeared at 3100 and 2930 cm^{-1}, but these decreased and disappeared in (a) and (b). This means that the TSA with the toluene group exists predominantly in rod-type PPY rather than in the grain-type, and there is stronger interaction between PPY and TSA. In an IR spectroscopy study

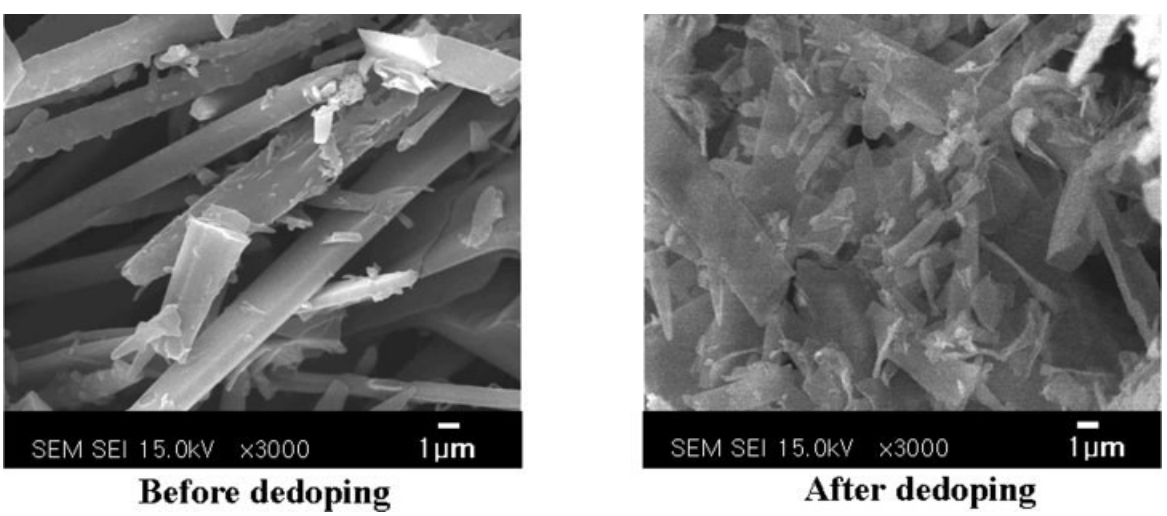

Figure 8 SEM images of PPY rod before and after dedoping with 3 mol/L of $NH_3 \cdot H_2O$.

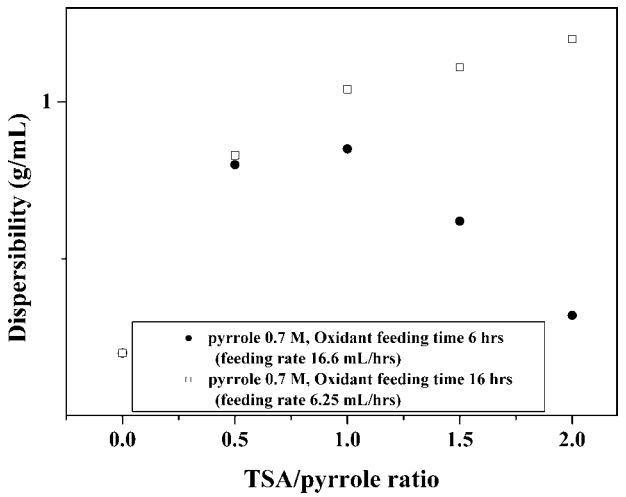

Figure 9 Effect of oxidant feed rate and time and molar ratio of TSA/pyrrole on the dispersibility of synthesized PPY doped with TSA.

carried out by Uyar et al., similar changes in peak intensity owing to the thermal degradation of TSA were recorded.[27]

Dedoping and redoping of PPY rod

To confirm the existence of TSA as dopant and the effect of dopping, base treatment was carried out. The PPY rod powder (0.5 g) was dedoped with 500 mL of $NH_3 \cdot H_2O$ (3 mol/L). And then the powder was redoped with 500 mL of HCl aqueous solution (3 mol/L). Each powder was dried at room temperature, and then solubilized into *m*-cresol with ultrasonification treatment. Figure 7 shows UV–vis spectra of each sample. By treatment with base, shift of the polaron peak to low wave length was observed. This could be evidence of dedoping PPY rod through neutralization of acid with base. On the contrary, the UV spectrum of the powder redoped with HCl exhibited a peak of π-π^* transition near 350 nm and polaron peak over 800 nm. To support the effect of TSA, the structure of dedoped PPY rod was investigated through the WAXD.[26] As shown in Figure 4(d), crystallinity exhibited by PPY rod decreased after dedoping with $NH_3 \cdot H_2O$. This phenomenon implies destruction of the crystalline structure and disappearance of high degree order and supports the premise of self assembly of rod morphology in PPY through TSA micelle formation. In addition, the changes of morphologies after dedoping were observed on SEM images in Figure 8. As a result, TSA in PPY have a significant effect on dopping of PPY as well as self crystallization of PPY rod.

Dispersity and miscibility with Nafion®

As determined in previous studies,[23,24] PPY doped with organic acid had high dispersity because of the hydrophilicity of the sulfonate group. As shown in Figure 9, when the small granular and rod forms of PPY doped with TSA were formed at a slow oxidant feed rate, the dispersity of PPY doped with TSA increased with an increase in TSA/PY molar ratio.

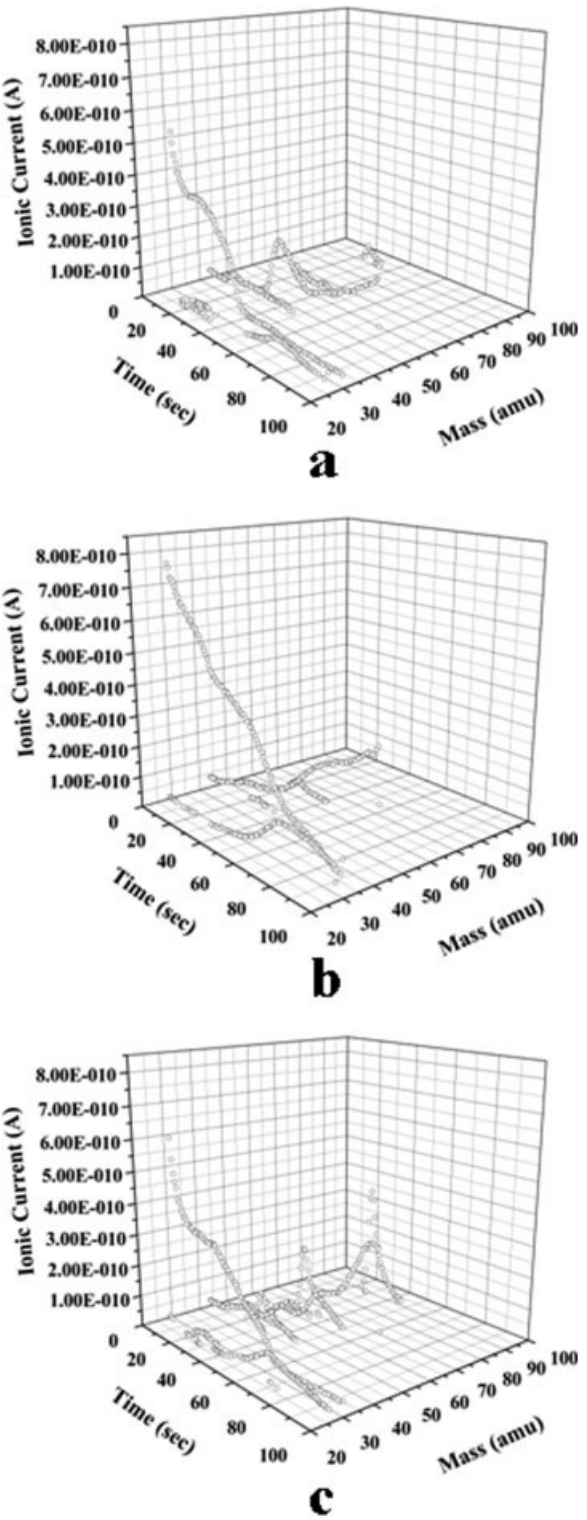

Figure 10 TGA/mass spectra of (a) rod-type, (b) grain-type, and (c) partially rod-type PPY doped with TSA.

TABLE I
Decomposition Temperature Ranges of Different Types of PPY (TSA)

Type of PPY (TSA)	Atomic molecular weight			
	28–29	48–49	31–32	43–44
Rod	530–870°C	240–460°C	Decrease continuously at whole region	Increase continuously at whole region
Partially rod	460–940°C	230–510°C		
Grain	340–990°C	180–420°C		
Elements assumed	$^{14}N^{15}N$, N_2	SO_3^+, SO_2	SO_2^+, SO_2. O_2^+, O_2S^+, H_2S, S^+, SO_2	$C_3H_7^+$, C*x*H*y*, $C_2H_3O^+$, C_2H_5OH

The dispersity of granular PPY doped with TSA increased from 0.83 g/100 mL to 1.04 g/100 mL in *m*-cresol. It is especially rod-type PPY exhibits relatively high dispersity in *m*-cresol, of $\sim$ 1.2 g/100 mL. To observe the dispersive stability, 1.2 g of PPY rod was solubilized into 100 mL *m*-cresol. The solution of PPY rod doped with TSA has dispersive stability for 48 h after initial dispersing. On the contrary, when a fast oxidant feed is used (16.6 mL/h), the dispersity of the resultant PPY doped with TSA decreased because of a low doping level of TSA due to coagulation of the PPY particles, and the PPY precipitated after 24 h.

Additional blending experiments were conducted, to determine miscibility with other commercial polymers and the stability of PPY rods after sonification. To investigate the miscibility of PPY rods and grains with Nafion®, a film of Nafion®/PPY was prepared by solution blending. The PPY rods had higher miscibility with Nafion® compared with the granular PPY.

Thermal stability

The thermal properties of each type of PPY doped with TSA are shown in Figure 10 and decomposition temperatures are given in Table I. The first weight loss between 100 and 120°C is caused by evaporation of water molecules of hydration of PPY. Considerable weight loss, as a result of the thermal decomposition of TSA, was observed from 200 to 400°C. Above 450°C the PY main chain decomposed and the PY rings opened. It was not possible to determine here which type of PPY doped with TSA is more stable thermally.

To determine the thermal decomposition mechanism of each type of PPY doped with TSA, careful analysis of the elements of gases arising from thermal decomposition were determined by TGA/mass analysis. On the TGA/mass spectra, the elements whose atomic molecular weight (amu) values were between 31 and 32 were assumed to represent SO_2 or O_2, and the ionic current decreased continuously. This means that TSA decomposes throughout the thermal decomposition and that the quantity of gas detected decreases gradually. On the other hand, the ionic current of the alkyl groups from 43 to 44 amu increased continuously. Detection of these alkyl groups is possible because only TSA decomposes at the initial temperature and the PY main chain decomposes later. Molecular mass (amu) values from 48 to 49 and those from 28 to 29 represent N_2 and SO_2, respectively. Gases from the different types of PPY doped with TSA are detected in different regions. When comparing rod-type to grain-type, N_2 and SO_2 gases develop at higher temperature in the rod-type than in grain-type. Thermal stability and decomposition temperatures depend on the crystallinity of the samples. As shown in Figure 4, the high crystallinity of the PPY rods delays decomposition of the PPY chain. Further, the data indicate that possibly both the PPY main chain decomposition and PY ring opening were delayed due to the TSA around the PPY matrix in rod-type PPY doped with TSA. This logic is reasonable, assuming that heat transfer proceeds from outside the TSA shell to the inner PPY matrix. Once decomposition of TSA was completed, then decomposition of the PPY commenced. Data obtained for N_2 gas for the partially rod-type PPY doped with TSA showed a decomposition temperature between the rod-type and grain-type. Consequently, formation of rod-type PPY doped with TSA arises from TSA emulsion formation, and the outer shell of TSA contributes positively toward delaying the thermal decomposition of the PPY conducting matrix. These results support the assumption that the PPY matrix is affected by a TSA layer, which is formed by a micelle forming mechanism. As a result, TSA accomplishes simultaneously the functions of a dopant, a surfactant, an interrupter that disturbs conductivity, and a barrier against outside heat.

CONCLUSION

In this study, to produce conducting fillers of good performance, various types of PPY doped with TSA were obtained by changing the conditions of polymerization. The shape of the PPY particles is mainly determined by the TSA/PY ratio and the oxidant feed rate. Particles of different shapes (rod, grain,

and partially rod) exhibit differences in morphology, electrical properties, dispersity, miscibility, and thermal properties. The electrical conductivity of PPY doped with TSA increased as the ratio of TSA/PY increased up to 1.0 and decreased when the ratio of TSA/PY exceed 1.0. However, if the oxidant feed was too slow, then rod-type morphology developed, and the decrease of electrical conductivity was relieved. PPY rods were produced under the following conditions: a slow feed rate (6.25 mL/h) and a high TSA/PY ratio (2.0). When compared with the grain-type, PPY rods exhibited high crystallinity, dispersity, miscibility and thermal stability.

References

1. Shirakawa, H.; Louis, E. J.; MacDiarmid, A. G.; Chiang, C. K.; Heeger, A. J. J Chem Soc Commun 1977, 577.
2. Kaynak, A. Fiber Polym 2001, 2, 171.
3. Lee, S. H.; Lee, D. H.; Lee, K. H.; Lee, C. W. Adv Funct Mater 2005, 15, 1495.
4. Shen, Y.; Wan, M. J Polym Sci 1997, 35, 3689.
5. Rhee, S. B.; Kim, H. K. J Kor Fib Soc 1984, 21, 466.
6. Narkis, M.; Haba, Y.; Segal, E.; Zilberman, M.; Titelman, G. I.; Siegmann, A. Polym Adv Technol 2000, 11, 665.
7. Deligöz, H.; Tieke, B. Macromol Mater Eng 2006, 291, 793.
8. Kim, S. H.; Jang, S. H.; Byun, S. W.; Lee, J. Y.; Joo, J. S.; Jeong, S. H.; Park, M. J. J Appl Polym Sci 1969, 2003, 87.
9. Park, J. C.; Kim, J. S. Macromol Res 2002, 10, 181.
10. Lee, Y. K.; Kim, J. S. Polymer (Korea) 1998, 22, 953.
11. Martin, C. R. Chem Mater 1996, 8, 1739.
12. Make, T.; Pienimaa, S.; Jussila, S.; Isotalo, H. Synth Met 1999, 101, 705.
13. Yussuf, A. A.; Sbarski, I.; Solomon, M.; Tran, N.; Hayes, J. P. J Mater Process Technol 2007, 189, 401.
14. Oh, K. W.; Park, H. J.; Kim, S. H. J Appl Polym Sci 2004, 91, 3659.
15. Kohut-Svelko, N.; Dinant, F.; Magana, S.; Clisson, G.; Francois, J.; Dagron-Lartigau, C.; Reynaud, S. Polym Int 2006, 55, 1184.
16. Zhang, Z.; Wei, Z.; Wan, M. Macromolecules 2002, 35, 5937.
17. Bajpai, V.; He, P.; Dai, L. Adv Funct Mater 2004, 14, 145.
18. Lee, K. H.; Cho, S. U.; Park, S. H.; Heeger, A. J.; Lee, C. W.; Lee, S. H. Nature 2006, 441, 65.
19. Shen, Y.; Wan, M. J Appl Polym Sci 1998, 68, 1277.
20. Song, M. K.; Kim, Y. T.; Kim, B. S.; Kim, J. W.; Char, K. H.; Rhee, H. W. Synth Met 2004, 141, 315.
21. Wallace, G. G.; Spinks, G. M.; Kane-Maguir, L. A. P.; Teasdale, P. R. Conductive Electroactive Polymers: Intelligent Materials Systems, 2nd ed.; CRC Press: Boca Raton, FL, 2003.
22. Rupprecht, L. Conductive Polymers and Plastics in Industrial Application; Plastics Design Library: New York, 1999.
23. Havinga, E. E.; Horssen, L. W. V.; Hoeve, W. T.; Wynberg, H.; Meijer, E. W. Polymer Bull 1987, 18, 277.
24. Myers, D. Surface, Interfaces, and Colloids: Principles and Applications, 2nd ed. Wiley V.C.H.: New York, 1999.
25. Chandrasekhar, P. Conducting polymers, Fundamentals and Applications: A Practical Approach, Kluwer Academic Publishers: Hingham, MA, 1999.
26. Liu, J.; Wan, M. Synth Met 2001, 124, 317.
27. Uyar, T.; Toppare, L.; Hacaloğlu, J. Synth Met 2001, 123, 335.